Original Research

Comparison of human lung cancer cell radiosensitivity after irradiations with therapeutic protons and carbon ions

Otilija D Keta[1], Danijela V Todorović[2], Tanja M Bulat[1], Pablo GA Cirrone[3], Francesco Romano[3], Giacomo Cuttone[3], Ivan M Petrović[1] and Aleksandra M Ristić Fira[1]

[1]Vinča Institute of Nuclear Sciences, University of Belgrade, Belgrade 11001, Serbia; [2]Faculty of Medical Sciences, University of Kragujevac, Kragujevac 34000, Serbia; [3]Laboratori Nazionali del Sud, Instituto Nazionale di Fisica Nucleare, Catania 95123, Italy
Corresponding author: Aleksandra M Ristić Fira. Email: aristic@vin.bg.ac.rs

Abstract

The aim of this study was to investigate effects of irradiations with the therapeutic proton and carbon ion beams in two non-small cell lung cancers, CRL5876 adenocarcinoma and HTB177 large cell lung carcinoma. The DNA damage response dynamics, cell cycle regulation, and cell death pathway activation were followed. Viability of both cell lines was lower after carbon ions compared to the therapeutic proton irradiations. HTB177 cells showed higher recovery than CRL5876 cells seven days following the treatments, but the survival rates of both cell lines were lower after exposure to carbon ions with respect to therapeutic protons. When analyzing cell cycle distribution of both CRL5876 and HTB177 cells, it was noticed that therapeutic protons predominantly induced G1 arrest, while the cells after carbon ions were arrested in G2/M phase. The results illustrated that differences in the levels of phosphorylated H2AX, a double-strand break marker, exist after therapeutic proton and carbon ion irradiations. We also observed dose- and time-dependent increase in the p53 and p21 levels after applied irradiations. Carbon ions caused larger increase in the quantity of p53 and p21 compared to therapeutic protons. These results suggested that various repair mechanisms were induced in the treated cells. Considering the fact that we have not observed any distinct change in the Bax/Bcl-2 ratio following irradiations, it seemed that different types of cell death were involved in the response to the two types of irradiations that were applied.

Keywords: Lung cancer, cell irradiation, protons, carbon ions, DNA damage, radiobiology

***Experimental Biology and Medicine* 2017; 242: 1015–1024. DOI: 10.1177/1535370216669611**

Introduction

Lung cancer is the leading cause of cancer-related deaths around the world. About 80% of all lung cancers are non-small cell lung cancers (NSCLC),[1] and despite the recent advances, prognosis for NSCLC patients remains poor. Radiotherapy plays a very important role in cancer therapy, either early on or in the late stages of the disease.[2,3]

Approximately 20,000 oncological patients per year are treated with high-energy photons.[4] It was previously demonstrated that protons are able to enhance biological effectiveness in cell killing,[5] due to the increased linear energy transfer (LET) in comparison with X- and gamma-rays.[6–8] Proton energy deposition pattern is well defined. At the end of the proton tracks, a localized peak, known as the Bragg peak, is produced.[9] For clinical and research applications, spread out Bragg peak (SOBP) is formed in order to achieve uniform dose at different depths throughout the tissue. Carbon ion therapy, that is another type of particle therapy, shows improved results compared to other types of radiotherapy, especially in the treatment of radio-resistant tumours.[10,11]

Ionizing radiation induces DNA double strand breaks (DSBs), which leads to the phosphorylation of histone H2AX (γH2AX).[12] γH2AX acts as a sensor and recruits other proteins involved in DNA damage response (DDR), which has a major role in ensuring chromosomal stability and controlling cell viability.[13] DDR machinery controls cell cycle progression, before or during DNA replication (G1/S and intra-S checkpoints) and before cell division (G2/M checkpoint).[14,15] If potential DNA damage is not adequately repaired by DNA damage sensors, transducers, mediators, and effectors, regulated cell death will be induced.[13,16]

Understanding the damage repair processes and anticancer therapy-triggered mechanisms of cell death is crucial in designing therapy for radio- and/or chemo-resistant cancers.[17] Radiation and other DNA-damaging agents exert their therapeutic effects in sensitive tumor cells through activation of apoptosis.[18] The best characterized proteins in apoptotic machinery belong to Bcl-2 family and they can either promote or antagonize cell survival.[19] Thus, proapoptotic Bax and antiapoptotic Bcl-2 proteins act through

competitive dimerization and whether the apoptosis will be initiated depends on the relative ratio of Bax–Bax homodimers to Bax–Bcl-2 heterodimers.[20] After DNA damage, expression of Bax and Bcl-2 rests on transcription activity of tumor-suppressor p53. Wild-type p53 coordinates cell cycle arrest, DNA repair, senescence, and apoptosis.[16] Loss of p53 results in genomic instability, aneuploidy, and polyploidy,[21] while mutant p53 interacts with the MRE11–Rad51–NSB complex, p73, and other proteins, promoting invasion, therapeutic resistance, and proliferation.[22,23]

It has been suggested that p53 mediates cell cycle control by inducing expression of p21. Following DNA damaging stimulus, p21 inhibits cyclin-dependent kinases leading to growth arrest in G1 or G2 phase of cell cycle.[15,24–26] Additionally, p53/p21 pathway is involved in senescence, programmed cell death, and transcription.[22,27]

The aim of this study was to investigate the effects of therapeutic protons and carbon ion irradiations on DDR dynamics, regulation of cell cycle, and activation of cell death in CRL5876 adenocarcinoma cells and undifferentiated HTB177 large cell lung carcinoma.

Material and methods

Cell culture

The human CRL5876 and HTB177 cell lines were obtained from the American Tissue Culture Collection (Rockville, MD, USA) and maintained as monolayer cultures in RPMI-1640 medium supplemented with 10% fetal bovine serum and penicillin/streptomycin (Sigma-Aldrich Chemie GmbH, Steinheim, Germany), under standard conditions at 37°C, in humidified atmosphere with 5% CO_2 (Heraeus, Hanau, Germany). For the cultivation of CRL5876 cells the culture medium was additionally supplemented with glucose and sodium pyruvate (Sigma-Aldrich, Germany) at the final concentrations of 4.5 mg/mL and 1 mM, respectively.

Irradiation conditions

Proton irradiations. The beam of the 62 MeV therapeutic proton SOBP of the Centro di Adro Terapia e Applicazioni Nucleari Avanzate treatment facility at the Istituto Nazionale di Fisica Nucleare (INFN), Laboratori Nazionali del Sud (LNS) in Catania in Italy, was used for irradiations. Cells were irradiated in the middle of SOBP where the relative dose applied was $100.0 \pm 1.6\%$ with the corresponding LET value of 4.7 ± 0.2 keV/μm. This irradiation position was achieved by interposing 16.3 mm thick Perspex plates (poly(methyl methacrylate) (PMMA)) between the final collimator and cell monolayer.[7,8] Reference dosimetry was performed using a plane-parallel PTW 34045 Markus ionization chamber calibrated according to International Atomic Energy Agency technical Report series (IAEA 2000) code of practice.[28] Single doses delivered to the cells were in the range of 0.5–8 Gy, at the dose rate of ~12 Gy/min. All irradiations were carried out in air, at room temperature or at ~0°C when experimental conditions required inhibition of repair processes.

Carbon ion irradiations. Exponentially growing CRL5876 and HTB177 cells were irradiated with the 62 MeV/n ^{12}C ion beam also at INFN—LNS in Catania, Italy. The position for irradiation within the Bragg curve was obtained by interposing Perspex plates (PMMA) of different thickness between the final collimator and the cell monolayer. The thickness of Perspex was 7.7 mm, giving relative doses of 49%. Reference dosimetry was performed as mentioned before. Irradiation doses applied were the same as for the SOBP protons, with the average dose rate of ~12 Gy/min. The corresponding LET value was calculated by numerical simulations carried out with the GEANT4 (GEometryANd Tracking) code and was 197 keV/μm.[29,30] As in the case of proton irradiation, cell monolayers were fixed vertically in a special device for irradiation, facing the horizontal beam. Since the range of the 62 MeV/n ^{12}C ions is short, with a very narrow Bragg peak, the precision of positioning of the cell samples was checked by placing GafChromic HS films (ISP Technologies, Wayne, New Jersey, USA) before and after each irradiation. Irradiations were carried out in air at room temperature or at ~0°C when experimental conditions required inhibition of repair processes.

Cell viability assay. For the colony assay, immediately after irradiation, cells were harvested by trypsinization (0.25% trypsin, Serva Feinbiochemica, Heidelberg, Germany) and seeded at a suitable number into the six-well plates. After the incubation at 37°C for seven days, cells were fixed with methanol (Zorka Pharma, Sabac, Serbia) and stained with 10% Giemsa solution (Alkaloid A.D., Skopje, Macedonia). More than 50 cells per colony were scored as a surviving cell. Survival was calculated by comparing the number of colonies in irradiated samples with untreated control. Sulforhodamine B (SRB) assay, designed to measure cellular protein content, was used for the determination of cell density. Solubilized SRB binds to the basic amino acids in the cellular proteins and the colorimetric measurements of the bound dye correspond to the total protein content, which in turn is correlated with the number of cells.[31,32] After irradiation cells were seeded in 96-well plates at a density of 3000 cells per well. After chosen incubation periods of 48 h and seven days, the cells were fixed with 10% trichloroacetic acid and stained with 0.4% SRB (Sigma-Aldrich Chemie GmbH, Steinheim, Germany) for 15 min. The excess dye was removed by washing with 1% acetic acid. The protein-bound dye was dissolved in 10 mM Tris base solution for absorbance determination at 550 nm, using a microplate reader (Wallac, VICTOR2 1420 Multilabel counter, PerkinElmer, Inc., USA).

Cell cycle analysis. Evaluation of the cell cycle distribution was performed on samples containing 1×10^6 cells. Cells were washed with phosphate buffered saline (PBS), fixed overnight with ice cold 70% ethanol, and incubated with 500 μg/mL RNase in PBS for 30 min at 37°C. Subsequently, cells were stained with 50 μg/mL propidium iodide (Sigma-Aldrich, Germany) and were analyzed by Partec CyFlow flow cytometer (Partec GmbH, Munster, Germany), using ModFit software.

Western blot analysis

Total proteins were extracted from the cells 30 min, 2, 6, 24, 48 h, and seven days after irradiations with therapeutic protons and carbon ion beams. Briefly, cells were collected, washed with PBS, and homogenized with buffer containing 150 mM NaCl, 50 mM Tris–HCl (pH 8.0), 1% Nonidet P-40 (NP-40), 0.1% sodium dodecyl sulfate (SDS), 0.5% sodium-deoxycholate, 1 mM ethylenediaminetetraacetic acid, 1 mM glycol ether diamine tetraacetic acid, 1 mM dithiothreitol, 1 mM Na_3VO_4, 5 μg/mL aprotinin, 5 μg/mL antipain, 5 μg/mL leupeptin, 0.5 mM phenylmethanesulphonylfluoride, NaF, β-glycerophosphate and sodium pyrophosphate. The lysate was centrifuged at 1700 *g* for 20 min at 4°C. Amount of proteins was quantified spectrophotometrically.[33] The samples were mixed with denaturizing buffer according to Laemmli and boiled for 5 min.[34] For the analysis of γH2AX 60 μg of proteins were loaded onto a 12% SDS-PAGE, while for the analysis of other proteins 20 μg were used. Following primary antibodies were applied: anti-γH2AX antibody (BioLegend, San Diego, USA), anti-p53, anti-p21, anti-Bax, and anti-Bcl-2 (Cell Signaling Technology Inc., MA, USA) and anti-β-actin antibody (Sigma-Aldrich Chemie GmbH, Germany) at 1:1000 dilution in PBS Tween 20 (PBST) with bovine serum albumin (BSA) (Sigma-Aldrich Chemie GmbH, Germany). Horseradish peroxidase (HRP)-conjugated anti-mouse antibody (Cell Signaling Technology, MA, USA) or anti-goat-HRP-linked antibody (BioLegend, USA) was used as secondary antibodies, diluted 1:5000 in PBST with BSA. The quantifications of the detected protein bands were performed using ImageJ software.

Statistical analysis

Duplicate measurements were obtained from each experiment and all experiments were repeated at least three times. Tukey's test in conjunction with a two-way ANOVA was used to compare effects between experimental groups (control, proton, and carbon ion irradiated cells). All analyses were done using GraphPad 6.0 Prism statistical software (San Diego, CA, USA). Results were considered statistically significant for $P < 0.05$. All data are expressed as mean ± standard error of mean.

Results

Effects of therapeutic protons and carbon ion beams on NSCLC cell viability

Irradiation dose ranges for both cell lines that were used in this study were determined according to their specific radiosensitivity by the clonogenic survival assays. For the CRL5876 cells the dose range was from 1 to 8 Gy while that for the HTB177 cells was from 0.5 to 5 Gy. The surviving fractions at 2 Gy for CRL5876 and HTB177 cells, after proton irradiations were 0.49 and 0.35, while those after exposure to carbon ions were 0.05 and 0.11, respectively (Figure 1).

Figure 2 shows the effects of therapeutic protons and carbon ions on CRL5876 cell viability 48 h and seven days after treatments. According to the results obtained, viability of CRL5876 cells was greatly reduced 48 h after exposure to therapeutic protons and was statistically significant ($P < 0.001$) at higher doses (4, 6, and 8 Gy) (Figure 2(a)). The dose dependence of CRL5876 cell viability was more pronounced after seven days, although slight recovery of irradiated cells was detected at lower doses (1 and 2 Gy) (Figure 2(b)). After exposure of CRL5876 cells to carbon ions, we detected transient stimulation of cell viability at 48 h. This stimulation was lost after seven days when the decrease in cell viability was below 50% (Figure 2(a) and (b)).

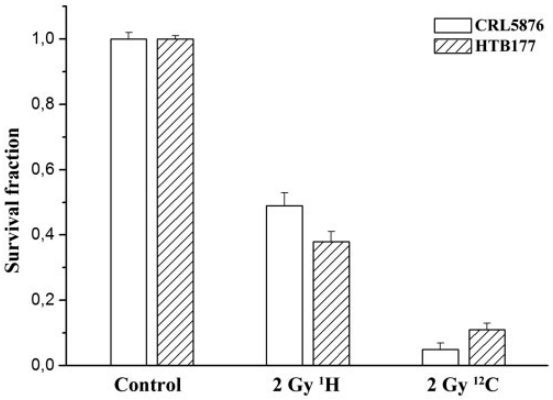

Figure 1 Comparison of clonogenic survival of CRL5876 and HTB177 cells after irradiations with 2 Gy of 62 MeV/n therapeutic (SOBP) protons and carbon ions. Error bars represent the standard error of the mean of three independent experiments

HTB177 cells showed reduction in viability 48 h after irradiations with therapeutic protons or carbon ions (Figure 2(c) and (d)). Nevertheless, seven days after the treatment with either of the two investigated irradiation types, the dose-dependent recovery of HTB177 cells can be noticed with the lowest percentage of recovery detected for the highest dose. Statistical differences between therapeutic protons and carbon ion irradiations at this time point have not been detected.

Changes in NSCLC cell cycle distribution after therapeutic proton and carbon ion irradiations

Irradiations with therapeutic protons increased percentage of CRL5876 cells in G1 phase which was accompanied by the reduction in S phase, when compared to untreated control, for all applied doses at 24 h. In this time point, carbon ions induced G2/M arrest in a dose-dependent manner (Figure 3(a)). In order to elucidate the long-term effects of therapeutic protons and carbon ion irradiation on cell cycle, two doses of 1 and 3 Gy were chosen and cells were analyzed after 48 h and seven days. The dose of 1 Gy was chosen as lower while that of 3 Gy was considered higher dose according to the survival data and the dose range for the two cell lines. The time point of 48 h after irradiation was selected for the assessment of cell death and following changes in protein levels, while that of seven days post-treatment was used for estimation of radiosensitivity and clonogenic survival.

Both protons and carbon ions increased the number of cells in G2/M phase of the cell cycle at 48 h and seven days

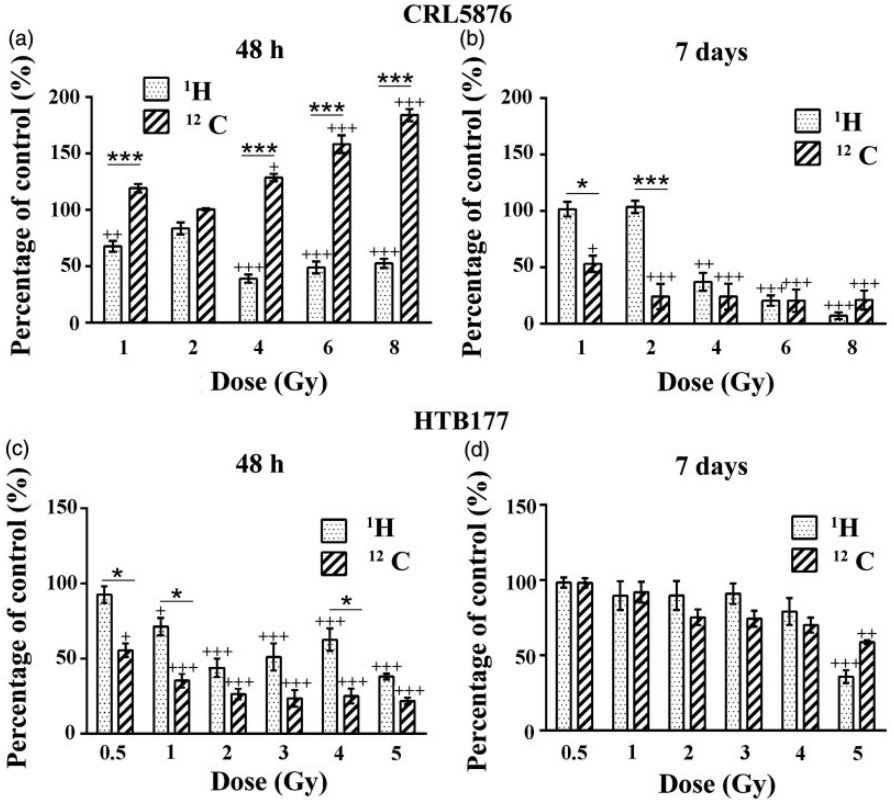

Figure 2 Changes in (a) CRL5876 and (b) HTB177 cell viability, 48 h and seven days after irradiations with SOBP protons (^{1}H) and carbon ions (^{12}C), obtained with SRB assay. For CRL5876 cells, applied doses were 1, 2, 4, 6, and 8 Gy, while for HTB177 they were 0.5, 1, 2, 3, 4, and 5 Gy. Results are presented as mean ± standard error of mean (SEM).
$^{+}$Statistical significance compared with the control, *Statistical significance SOBP protons versus carbon ions: $^{+}$,*$0.01 < P < 0.05$; $^{++}$, **$0.001 < P < 0.01$; $^{+++}$,***$P < 0.001$

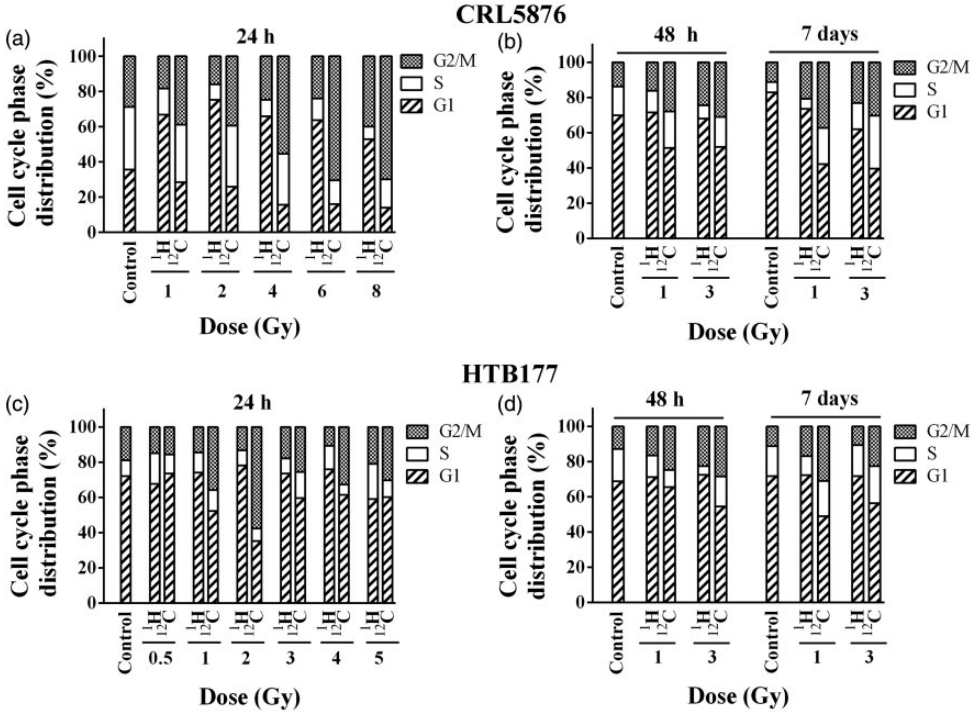

Figure 3 Cell cycle distribution of (a) CRL5876 and (b) HTB177 cells 24, 48 h, and seven days after irradiations with SOBP protons and carbon ions. Doses applied were 1, 2, 4, 6, and 8 Gy for CRL5876 cells and 0.5, 1, 2, 3, 4, and 5 Gy for HTB177 cells, for measurements after 24 h. Cell cycle distribution was analyzed after irradiations with 1 and 3 Gy of both SOBP protons and carbon ions, for both cell lines, at 48 h and seven days

(Figure 3(b)). This increase was dose dependent and it was more pronounced after irradiations with carbon ions when comparing with the same doses of therapeutic protons. Moreover, in analyzed samples carbon ions provoked the increase of S phase at seven days.

Irradiations with therapeutic protons did not produce any specific change in the HTB177 cell cycle distribution 24 h after the treatment (Figure 3(c)). Still, exposure to carbon ion beams for the doses higher than 0.5 Gy increased the number of cells in G2/M phase, followed by the decrease in G1 phase (Figure 3(c)).

Irradiations of HTB177 cells with therapeutic protons at 48 h provoked the dose-dependent G2/M arrest with reduction of cell number in S phase for both applied doses. At the same time point, carbon ions induced G2/M arrest with the decreased number of cells in G1 phase in comparison with the control and therapeutic proton irradiations (Figure 3(d)). Higher percentage of cells in G2/M phase was detected in samples irradiated with carbon ions than in samples irradiated with therapeutic protons, seven days after irradiation (Figure 3(d)). G2/M block was more pronounced seven days after the treatment with carbon ions but the dose dependence was not observed (Figure 3).

Protein expression in NSCLC cells after therapeutic proton or carbon ion irradiations

The dose-dependent effects of irradiations were followed 2 h after exposure of NSCLC cells to the two radiation types, while the time-dependent changes in protein levels were analyzed 30 min, 2, 6, and 24 h after cell irradiations with the single dose of 4 Gy. Based on the results of survival and viability tests this dose was considered to be optimal for Western blot assay. Changes of protein levels (p53, p21, γH2AX, Bax, and Bcl-2) in CRL5876 cells, after irradiations with therapeutic proton and carbon ion beams are presented in Figure 4.

According to the results obtained, 2 h after irradiation, both therapeutic protons and carbon ions significantly increased the level of p53 protein compared to the control ($P < 0.001$). Higher amount of p53 was detected in samples that were irradiated with carbon ions than in those irradiated with therapeutic protons (Figure 4(a)). Expression of p53 after irradiations with 4 Gy of both irradiation types increased in time, reaching the highest values at 24 h time point (Figure 4(b)).

Significant differences in the expression of p53 are observed 6 and 24 h after irradiations with therapeutic protons, as compared to the control. Regarding the treatment with carbon ions, the same effect is obtained after 2, 6, and 24 h (Figure 4(a) and (b)). Statistical difference between the p53 levels in CRL5876 cells exposed to different types of irradiations is present at higher doses (4, 6, and 8 Gy) 2 h after the treatment. Changes of level of p53 between therapeutic protons and carbon ions are significant at 2, 6, and 24 h postirradiation.

The level of p21 protein increased in CRL5876 cells at all doses, 2 h after irradiation, for both irradiation types (Figure 4(c)). Significant changes of the protein level were detected for higher doses (4, 6, and 8 Gy) after therapeutic protons and carbon ion irradiations, in comparison to the control. When relating the effects of the two irradiation types, there is no significant difference between protons and carbon ion irradiations regarding the increase of the dose, but as regards different time points, carbon ions induce considerable increase of p21 compared to the therapeutic protons in all time points.

Both irradiation types induced the increase of phosphorylated histone H2AX in CRL5876 cells, at all doses applied. In comparison with the control, treatment with therapeutic protons causes significant effect at higher doses (4 Gy, $P < 0.01$; 6 and 8 Gy, $P < 0.001$). After irradiation with carbon ions change was significant ($P < 0.001$) for the doses of 4, 6, and 8 Gy, compared to the control. Despite the changes induced by the treatments, statistically significant difference was found only after exposure to the highest dose of 8 Gy of carbon ions, compared to the same dose of therapeutic protons (Figure 4(e)). The level of phosphorylated H2AX reached maximum 2 h after irradiation with 4 Gy of therapeutic protons and carbon ions (Figure 4(f)). Also, at 24 h, γH2AX levels in samples treated with different irradiation types decreased to the level similar to the one measured in the control sample.

Bax/Bcl-2 ratio did not change 2 h after treatment of CRL5876 cells with therapeutic protons or carbon ion irradiation in comparison to the control. Also, there was no significant difference in Bax/Bcl-2 ratio induced by different irradiation types (Figure 4(g) and (h)).

For the HTB 177 cells clonogenic assay was performed in the dose range from 0.5 to 5 Gy showing strong cell inactivation at higher doses. Therefore, for this cell line we have selected only two irradiation doses (1 and 3 Gy). They represent lower and higher dose causing changes at the level of protein expression measurable by Western blot method (Figure 5). The level of p53 increased with the rise of the dose 2 h after irradiations with either therapeutic protons or carbon ions (Figure 5(a)). Moreover, after irradiations with the dose of 4 Gy of therapeutic protons or carbon ions, the level of p53 increased significantly during the period of 24 h ($P < 0.001$) (Figure 5(b)). When comparing the effects of the two irradiation types, there were no differences in the p53 levels (Figure 5(a) and (b)). Similarly, we found the dose- and time-dependent increase in the expression of p21 for both irradiation types (Figure 5(c) and (d)). Although 4 Gy of carbon ions had greater effect on the expression of p21 than therapeutic protons, statistically significant differences are found only at 6 and 24 h after irradiation ($P < 0.01$, $P < 0.001$) (Figure 5(d)). Both carbon ions and therapeutic protons enhanced the expression of phosphorylated H2AX in a dose-dependent manner (Figure 5(e)). Still, carbon ions increased the levels of γH2AX more than therapeutic protons ($P < 0.001$). The maximal expression of γH2AX after 4 Gy of both irradiation types was found after 2 h (Figure 5(f)). Statistically significant increase in Bax/Bcl-2 ratio was noticed only 24 h after treatment with carbon ions, as compared either with the control or with therapeutic protons ($P < 0.001$) (Figure 5(g) and (h)).

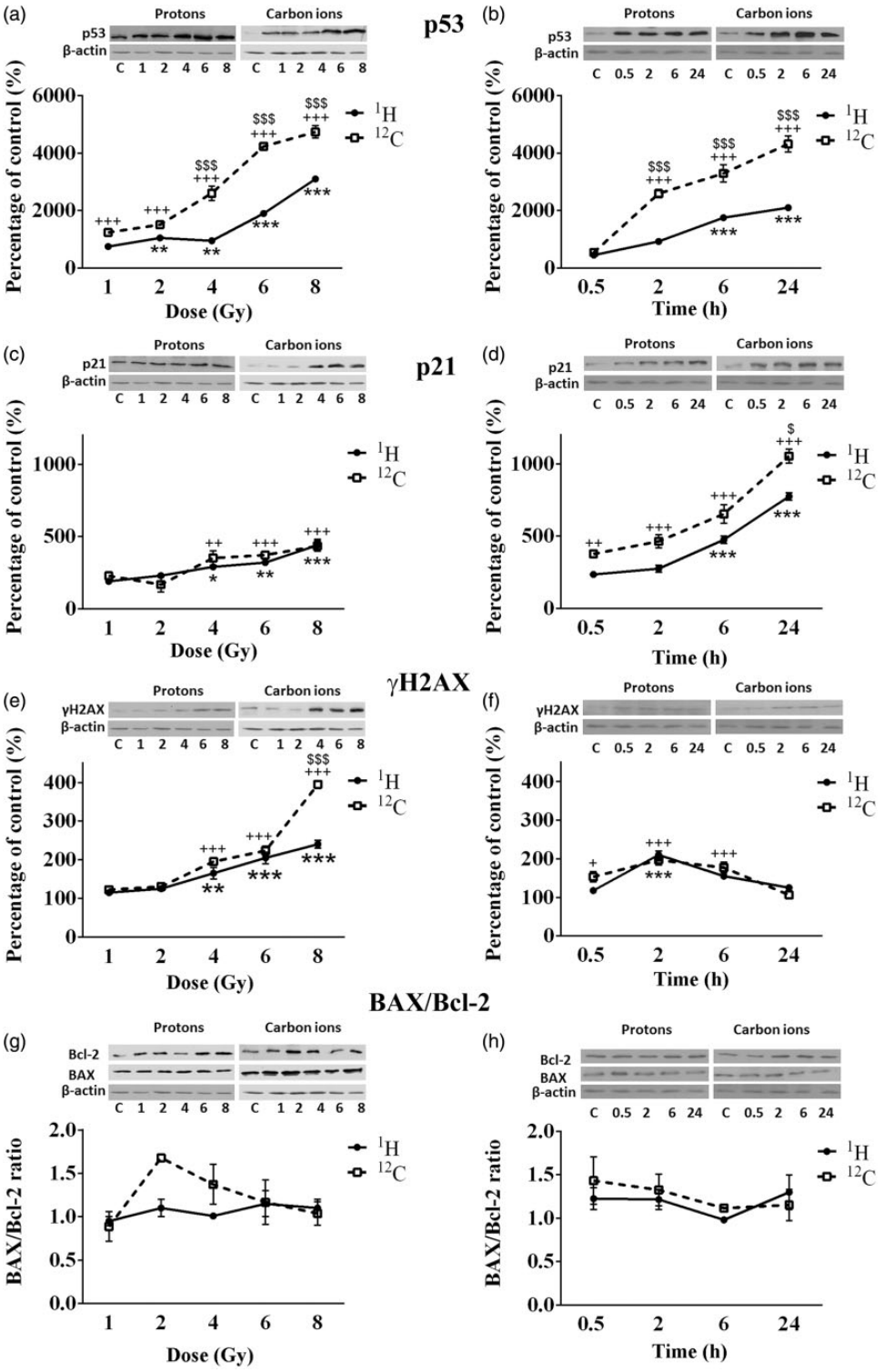

Figure 4 Changes in levels of p53 (a and b), p21 (c and d), γH2AX (e and f), BAX and Bcl-2 (g and h) in CRL5876 cells. Dose-dependent changes were followed 2 h after irradiations with different doses (1, 2, 4, 6, and 8 Gy) of SOBP protons and carbon ions. Time-dependent changes were followed at four time points (0.5, 2, 6, and 24 h) after irradiations with 4 Gy of SOBP protons and carbon ions. Results are presented as mean ± standard error of mean (SEM).
*Statistical significance SOBP compared with the control, $^{+}$Statistical significance carbon ions compared with the control, $^{\$}$Statistical significance SOBP versus carbon ions: *,$^{+}$,$^{\$}0.01 < P < 0.05$; **,$^{++}$,$^{\$\$}0.001 < P < 0.01$; ***,$^{+++}$,$^{\$\$\$}P < 0.001$

Discussion

Although radiotherapy is being widely used for locally advanced NSCLC, the outcomes are still not satisfactory.[2] Besides conventional radiotherapy, charged particles (protons and carbon ions) are also being used in the treatments of malignant tumours.[10,35] Due to the superior dosimetric characteristics of protons over photons, proton radiotherapy is shown to be useful in treatment of different

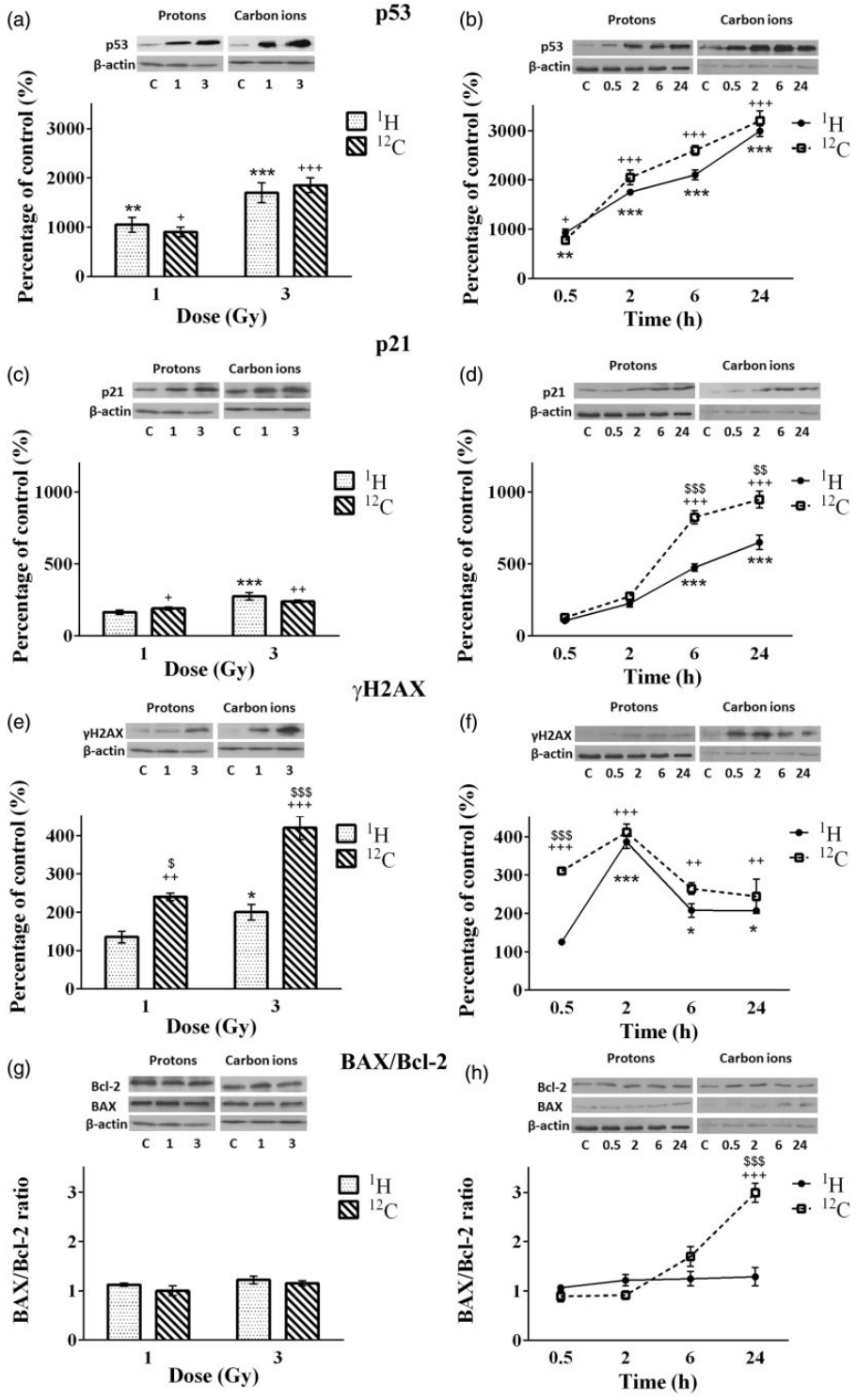

Figure 5 Changes in p53 (a and b), p21 (c and d), γH2AX (e and f), BAX and Bcl-2 (g and h) levels in HTB177 cells. Dose-dependent changes were followed 2 h after irradiation with different doses (1 and 3 Gy) of SOBP protons and carbon ions. Dynamic changes in the level of proteins were analyzed after irradiations with 4 Gy with SOBP protons and carbon ions. Time points are 0.5, 2, 6, and 24 h. Results are presented as mean ± standard error of mean (SEM).
*Statistical significance SOBP compared with the control, $^+$Statistical significance carbon ions compared with the control, $^\$$ Statistical significance SOBP versus carbon ions: $^*,^+,^\$0.01 < P < 0.05$; $^{**},^{++},^{\$\$}0.001 < P < 0.01$; $^{***},^{+++},^{\$\$\$}P < 0.001$

stages of NSCLC. The main advantage of proton radiotherapy over conventional radiotherapy is precise dose delivery which reduces the adverse effects of the treatment, thus diminishing the potential risk for healthy tissues, like lungs, heart, esophagus, and spinal cord.[36] According to the data obtained from clinical studies involving NSCLC patients, carbon ion irradiation shows better effects than proton irradiation. Still the use of carbon ions is under investigation.[11]

The aim of this study was to investigate the effects of therapeutic proton and carbon ion irradiations on the two NSCLC cell lines in terms of cell survival and viability, cell cycle distribution, and DNA damage. The CLR5876 and HTB177 cancer cells were chosen within NSCLC as example of two distinctive histological forms of NSCLC (adenocarcinoma and large cell lung cancer, respectively).[37] Both cell lines are derived from metastatic sites, thus representing severe stage of the disease. Cells can be classified according to their radiosensitivity through SF2 values (cell survival at 2 Gy). Thus, cells can be considered as radioresistant when having SF2 values higher than 0.6, and radiosensitive for the SF2 lower than 0.5.[38] According to this classification, HTB177 cells with SF2 of 0.64 belong to radioresistant group of cells.[39–42] The CRL 5876 cells also showed similar level of sensitivity to gamma irradiation, having SF2 value of 0.61.[43] In this study we displayed that protons and carbon ions further increased radiosensitivity of both cell lines (Figure 1).

Irradiation can induce the activation of signaling pathways in cancer cells, for example by activation of tyrosine kinase growth factor receptors, such as the epidermal growth factor receptor and serine-threonine kinase (Akt), as noticed in head and neck squamous cell cancers, NSCLC, and cervical cancers. Activation of these pathways can be demonstrated by the increased viability, cell proliferation rates, and survival after irradiation.[44,45] In our study, carbon ions induced transient stimulation of CRL5876 cell viability 48 h after the treatment, but at longer time period of seven days, greater decrease in viability of both cell lines was found in comparison with SOBP protons. HTB177 cells showed better recovery than CRL5876 cells seven days after irradiations (Figure 2).

Phosphorylated histone, γH2AX, is a known DSB marker, and measuring dynamic changes of this protein may allow understanding of cellular behavior regarding DSB reparation in response to irradiation. Different types of irradiations can lead to formation of different types of DNA strand breaks, including simple DSBs, two-ended DSBs, one-ended DSBs, as well as single-strand breaks. Furthermore, Liu *et al*. and Hall reported that the same number of DNA breaks can be detected when different irradiation types are applied.[46,47]

Previous studies demonstrated that carbon ion irradiation triggers higher complexity of DNA damage in comparison with other types of irradiations. This complexity can influence different processes that follow irradiations in the later stages.[48,49] Results obtained in this study show that differences in phosphorylation level of H2AX exist after SOBP proton and carbon ion treatments, for both cell lines, at different time points or applied doses. Also, differences in the cells cycle phase distribution after these two types of irradiations were observed. Our results, showing that G2/M arrest is the most pronounced effect of carbon ion treatment, indicate that complex DNA DSBs are created in response to this type of irradiation (Figure 3). Nonhomologous end joining has been indicated as the most common repair mechanism in the simple radiation-induced DSB repair, and its activation leads to arrest in G1 phase of the cell cycle. On the other hand, homologous recombination is possible when sister chromatids are present, during S and G2 phase. Also, it is specific to complex DSB repair (one- or two-ended DSB).[50,51] Considering these facts, the results suggest that various repair mechanisms are involved in response to the treatments with SOBP protons and carbon ions.

Cell response to irradiation is a consequence of a complex interplay between DNA DSB repair proteins and p53 protein. Moreover, p53 regulates cell processes, which influence cell cycle by inducing cell cycle arrest at specific points until the DNA damage is repaired.[52] The results we obtained agree with these data, showing that in both cell lines, there is a dose-dependent and time-dependent increase in p53 expression levels, after both types of irradiation (Figure 4(a) and (b) and 5(a) and (b)). We also found time- and dose-dependent increase in p21 after application of both irradiation types. Higher expression of p53 and p21 was found after carbon ions. The increase of Bax/Bcl-2 ratio is typical for apoptosis.[53] Zong and Thompson have showed that different doses of the same cell death stimulus can trigger different cell death pathways. Thus, lower doses can induce apoptosis, while higher doses can trigger necrosis or other cell death pathways.[54] Furthermore, the agents that can induce formation of reactive oxygen species induce autophagy.[55,56] Multifunctional protein p21, apart from its role in cell cycle regulation, is involved in regulation of nonapoptotic cell death (i.e. senescence).[57] Considering the fact that we have not observed a pronounced change in Bax/Bcl-2 ratio after both irradiation treatments and that an increase in p21 expression over time is found, it can be suggested that different types of cell death are involved in the response to the SOBP proton or carbon ion irradiations.

Recently, a study indicated the necessity of preforming radiosensitization of NSCLC prior to irradiation treatment.[58] In order to apply the combined therapies in the best possible way, it is necessary to further investigate DDR machinery. The results we presented here indicate that carbon ions were superior to SOBP protons in cell inactivation of both analyzed NSCLC cell lines, which was confirmed by results from cell cycle analysis and key regulatory proteins involved in DDR. Still, in order to get better insights in response of cancer cells to radiation treatments more profound analysis is needed. This would provide data necessary for the improvement of cancer therapy.

Authors' contributions: All authors participated in the design, interpretation of the studies and analysis of the data and review of the manuscript; IMP, PGAC, FR, and GC conducted the physics part of experiments, while ODK, DVT, TMB, and AMRF conducted the biological part of experiments; ODK, DVT, and TMB wrote the manuscript.

ACKNOWLEDGEMENTS

The research leading to these results has received funding from the European Union Seventh Framework Programme FP7/2007-2013 under Grant Agreement nÂ° 262010-ENSAR. The EC is not liable for any use that can be made on the information contained herein. This work was also financially supported by the Ministry of Education, Science and Technological

Development of Serbia (grants 173046 and 171019) and by Istituto Nazionale di Fisica Nucleare, Laboratori Nazionali del Sud, Italy.

DECLARATION OF CONFLICTING INTERESTS

The author(s) declared no potential conflicts of interest with respect to the research, authorship, and/or publication of this article.

REFERENCES

1. Siegel R, DeSantis C, Virgo K, Stein K, Mariotto A, Smith T, Cooper D, Gansler T, Lerro C, Fedewa S, Lin C, Leach C, Cannady RS, Cho H, Scoppa S, Hachey M, Kirch R, Jemal A, Ward E. Cancer treatment and survivorship statistics, 2012. *CA Cancer J Clin* 2012;**62**:220–41.
2. DeSantis CE, Lin CC, Mariotto AB, Siegel RL, Stein KD, Kramer JL, Alteri R, Robbins AS, Jemal A. Cancer treatment and survivorship statistics, 2014. *CA Cancer J Clin* 2014;**64**:252–71.
3. Gao W, Liu L, Lu X, Shu Y. Circulating microRNAs: possible prediction biomarkers for personalized therapy of non-small-cell lung carcinoma. *Clin Lung Cancer* 2011;**12**:14–17.
4. Amaldi U, Kraft G. Radiotherapy with beams of carbon ions. *Rep Prog Phys* 2005;**68**:1861–82.
5. Paganetti H, Niemierko A, Ancukiewicz M, Gerweck LE, Goitein M, Loeffler JS, Suit HD. Relative biological effectiveness (RBE) values for proton beam therapy. *Int J Radiat Oncol Biol Phys* 2002;**53**:407–21.
6. Goodhead DT. Energy deposition stochastics and track structure: what about the target? *Radiat Prot Dosimetry* 2006;**122**:3–15.
7. Petrovic I, Ristic-Fira A, Todorovic D, Valastro L, Cirrone P, Cuttone G. Radiobiological analysis of human melanoma cells on the 62 MeV CATANA proton beam. *Int J Radiat Biol* 2006;**82**:251–65.
8. Petrovic I, Ristic-Fira A, Todorovic D, Koricanac L, Valastro L, Cirrone P, Cuttone G. Response of a radioresistant human melanoma cell line along the proton spread-out Bragg peak. *Int J Radiat Biol* 2010;**86**:742–51.
9. Karger CP, Jäkel O. Current status and new developments in ion therapy. *Strahlenther Onkol* 2007;**183**:295–300.
10. Fokas E, Kraft G, An H, Engenhart-Cabillic R. Ion beam radiobiology and cancer: time to update ourselves. *Biochim Biophys Acta* 2009;**1796**:216–29.
11. Demizu Y, Fujii O, Iwata H, Fuwa N. Carbon ion therapy for early-stage non-small-cell lung cancer. *Biomed Res Int* 2014;**2014**:727962.
12. Vignard J, Mirey G, Salles B. Ionizing-radiation induced DNA double-strand breaks: a direct and indirect lighting up. *Radiother Oncol* 2013;**108**:362–369.
13. Lavin MF. ATM and the Mre11 complex combine to recognize and signal DNA double-strand breaks. *Oncogene* 2007;**26**:7749–58.
14. Celeste A, Petersen S, Romanienko PJ, Fernandez-Capetillo O, Chen HT, Sedelnikova OA, Reina-San-Martin B, Coppola V, Meffre E, Difilippantonio MJ, Redon C, Pilch DR, Olaru A, Eckhaus M, Camerini-Otero RD, Tessarollo L, Livak F, Manova K, Bonner WM, Nussenzweig MC, Nussenzweig A. Genomic instability in mice lacking histone H2AX. *Science* 2002;**296**:922–27.
15. Bartek J, Lukas J. Mammalian G1- and S-phase checkpoints in response to DNA damage. *Curr Opin Cell Biol* 2001;**13**:738–47.
16. Collavin L, Lunardi A, Del Sal G. p53-family proteins and their regulators: hubs and spokes in tumor suppression. *Cell Death Differ* 2010;**17**:901–11.
17. Hassan M, Watari H, AbuAlmaaty A, Ohba Y, Sakuragi N. Apoptosis and molecular targeting therapy in cancer. *Biomed Res Int* 2014;**2014**:150845.
18. Schmidt-Ullrich RK. Molecular targets in radiation oncology. *Oncogene* 2003;**22**:5730–33.
19. Raisova M, Hossini AM, Eberle J, Riebeling C, Wieder T, Sturm I, Daniel PT, Orfanos CE, Geilen CC. The Bax/Bcl-2 ratio determines the susceptibility of human melanoma cells to CD95/Fas-mediated apoptosis. *J Invest Dermatol* 2001;**117**:333–40.
20. Reed JC. Bcl-2 and the regulation of programmed cell death. *J Cell Biol* 1994;**124**:1–6.
21. Prives C, Lowe SW. Cancer: mutant p53 and chromatin regulation. *Nature* 2015;**525**:199–200.
22. Harris SL, Levine AJ. The p53 pathway: positive and negative feedback loops. *Oncogene* 2005;**24**:2899–908.
23. Freed-Pastor WA, Prives C. Mutant p53: one name, many proteins. *Genes Dev* 2012;**26**:1268–86.
24. Taylor WR, Stark GR. Regulation of the G2/M transition by p53. *Oncogene* 2001;**20**:1803–15.
25. Liu G, Lozano G. p21 stability: linking chaperones to a cell cycle checkpoint. *Cancer Cell* 2005;**7**:113–14.
26. Gottifredi V, McKinney K, Poyurovsky MV, Prives C. Decreased p21 levels are required for efficient restart of DNA synthesis after S phase block. *J Biol Chem* 2004;**279**:5802–10.
27. Cazzalini O, Dona F, Savio M, Tillhon M, Maccario C, Perucca P, Stivala LA, Scovassi AI, Prosperi E. p21CDKN1A participates in base excision repair by regulating the activity of poly(ADP-ribose) polymerase-1. *DNA Repair (Amst)* 2010;**9**:627–35.
28. Absorbed dose determination in external beam radiotherapy: an international code of practice for dosimetry based on standards of absorbed dose to water. *IAEA Tech Rep Ser* 2001;**398**:135–50
29. Romano F, Cirrone GA, Cuttone G, Rosa FD, Mazzaglia SE, Petrovic I, Fira AR, Varisano A. A Monte Carlo study for the calculation of the average linear energy transfer (LET) distributions for a clinical proton beam line and a radiobiological carbon ion beam line. *Phys Med Biol* 2014;**59**:2863–82.
30. *GEANT4: detector description and simulation tool.* CERN Program Library, 1998.
31. Vichai V, Kirtikara K. Sulforhodamine B colorimetric assay for cytotoxicity screening. *Nat Protoc* 2006;**1**:1112–16.
32. Skehan P, Storeng R, Scudiero D, Monks A, McMahon J, Vistica D, Warren JT, Bokesch H, Kenney S, Boyd MR. New colorimetric cytotoxicity assay for anticancer-drug screening. *J Natl Cancer Inst* 1990;**82**:1107–12.
33. Lowry OH, Rosebrough NJ, Farr AL, Randall RJ. Protein measurement with the Folin phenol reagent. *J Biol Chem* 1951;**193**:265–75.
34. Laemmli UK. Cleavage of structural proteins during the assembly of the head of bacteriophage T4. *Nature* 1970;**227**:680–85.
35. Kamada T, Tsujii H, Blakely EA, Debus J, De Neve W, Durante M, Jakel O, Mayer R, Orecchia R, Potter R, Vatnitsky S, Chu WT. Carbon ion radiotherapy in Japan: an assessment of 20 years of clinical experience. *Lancet Oncol* 2015;**16**:E93–E100.
36. Langendijk JA, Lambin P, De Ruysscher D, Widder J, Bos M, Verheij M. Selection of patients for radiotherapy with protons aiming at reduction of side effects: the model-based approach. *Radiother Oncol* 2013;**107**:267–73.
37. Gazdar AF. Should we continue to use the term non-small-cell lung cancer? *Ann Oncol* 2010;**21**:vii225–29.
38. Matthews Q, Jirasek A, Lum JJ, Brolo AG. Biochemical signatures of *in vitro* radiation response in human lung, breast and prostate tumour cells observed with Raman spectroscopy. *Phys Med Biol* 2011;**56**:6839–55.
39. Eschrich S, Zhang H, Zhao H, Boulware D, Lee JH, Bloom G, Torres-Roca JF. Systems biology modeling of the radiation sensitivity network: a biomarker discovery platform. *Int J Radiat Oncol Biol Phys* 2009;**75**:497–505.
40. Amorino GP, Freeman ML, Choy H. Enhancement of radiation effects in vitro by the estrogen metabolite 2-methoxyestradiol. *Radiat Res* 2000;**153**:384–91.
41. Park SY, Kim YM, Pyo H. Gefitinib radiosensitizes non-small cell lung cancer cells through inhibition of ataxia telangiectasia mutated. *Mol Cancer* 2010;**9**:22
42. Sak A, Stuschke M, Wurm R, Schroeder G, Sinn B, Wolf G, Budach V. Selective inactivation of DNA-dependent protein kinase with antisense oligodeoxynucleotides: consequences for the rejoining of radiation-induced DNA double-strand breaks and radiosensitivity of human cancer cell lines. *Cancer Res* 2002;**62**:6621–24.

43. Keta O, Bulat T, Korićanac L, Žakula J, Cuttone G, Privitera G, Petrović I, Ristić-Fira A. Radiosensitization of non-small cell lung carcinoma by EGFR inhibition. *NT&RP* 2014;**29**:233–41.
44. Goodhead DT. Initial events in the cellular effects of ionizing radiations: clustered damage in DNA. *Int J Radiat Biol* 1994;**65**:7–17.
45. Terato H, Ide H. Clustered DNA damage induced by heavy ion particles. *Biol Sci Space* 2004;**18**:206–15.
46. Liu Q, Ghosh P, Magpayo N, Testa M, Tang S, Gheorghiu L, Biggs P, Paganetti H, Efstathiou JA, Lu HM, Held KD, Willers H. Lung cancer cell line screen links fanconi anemia/BRCA pathway defects to increased relative biological effectiveness of proton radiation. *Int J Radiat Oncol Biol Phys* 2015;**91**:1081–89.
47. Hall EJ. The relative biological efficiency of X-rays generated at 220 Kvp and gamma radiation from a Cobalt 60 therapy unit. *Br J Radiol* 1961;**34**:313–17.
48. Morgan MA, Lawrence TS. Molecular pathways: overcoming radiation resistance by targeting DNA damage response pathways. *Clin Cancer Res* 2015;**21**:2898–904.
49. Warters RL, Adamson PJ, Pond CD, Leachman SA. Melanoma cells express elevated levels of phosphorylated histone H2AX foci. *J Invest Dermatol* 2005;**124**:807–17.
50. Davis AJ, Chen DJ. DNA double strand break repair via non-homologous end-joining. *Transl Cancer Res* 2013;**2**:130–43.
51. Kastan MB, Bartek J. Cell-cycle checkpoints and cancer. *Nature* 2004;**432**:316–23.
52. Lee JM, Bernstein A. p53 mutations increase resistance to ionizing radiation. *Proc Natl Acad Sci USA* 1993;**90**:5742–46.
53. Filippovich I, Sorokina N, Lisbona A, Chérel M, Chatal J. Radiation-induced apoptosis in human myeloma cell line increases BCL-2/BAX dimer formation and does not result in BAX/BAX homodimerization. *Int J Cancer* 2001;**92**:651–60.
54. Zong WX, Thompson CB. Necrotic death as a cell fate. *Gene Dev* 2006;**20**:1–15.
55. Azad MB, Chen YQ, Gibson SB. Regulation of autophagy by reactive oxygen species (ROS): implications for cancer progression and treatment. *Antioxid Redox Sign* 2009;**11**:777–90.
56. Karna P, Zughaier S, Pannu V, Simmons R, Narayan S, Aneja R. Induction of reactive oxygen species-mediated autophagy by a novel microtubule-modulating agent. *J Biol Chem* 2010;**285**:18737–48.
57. Kong Y, Cui H, Ramkumar C, Zhang H. Regulation of senescence in cancer and aging. *J Aging Res* 2011;**2011**:963172.
58. Kubo N, Noda SE, Takahashi A, Yoshida Y, Oike T, Murata K, Musha A, Suzuki Y, Ohno T, Takahashi T, Nakano T. Radiosensitizing effect of carboplatin and paclitaxel to carbon-ion beam irradiation in the non-small-cell lung cancer cell line H460. *J Radiat Res* 2015;**56**:229–38.

(Received April 8, 2016, Accepted August 23, 2016)